Periyayya Uthirakumar, H. Nam, SeungHee Wo, Eun-Kyung Suh and Chang-Hee Hong
**A Catalyst-free Approach to Prepare Nano to Microstructures of GaN from a Single Molecular Complex Precursor** JKPS 2009 55:59-63. [초록]

KuangYao Chen, C.-T. Liang, N. Aoki, Y. Ochiai, K.A. Cheng, Li-Hung Lin, C.F. Huang, Yu-Ru Li, YenShung Tseng, Chun-Kai Yang, Po-Tsun Lin, Jau-Yang Wu and Sheng-Di Lin
**Probing Insulator-quantum Hall Transitions by Current Heating** JKPS 2009 55:64-67. [초록]

Hee-Suk Chung, SeulCham Kim, DoHyun Kim, JiWoo Kim, O-Jong Kwon, Chan Park and KyuHwan Oh
**$₩bm₩beta$-Ga$_{2}$O$_{3}$ Nanowires and Nanobelts Synthesized byUsing GaAs Powder Evaporation** JKPS 2009 55:68-71. [초록]

Jae-Hong Kwon, Sang-Il Shin, Chang-Hoon Kim, In-Kyu You, Gyeong-Ik Cho and Byeong-Kwon Ju
**Flexible Organic Thin-film Transistors for Photodetectors** JKPS 2009 55:72-75. [초록]

Yungjun Kim, Sanghoon Lee, M. Dobrowolska and J.K. Furdyna
**Spin Phenomena of CdZnSe Self-assembled Quantum Dots Investigatedby Magneto-photoluminescence** JKPS 2009 55:76-79. [초록]

C.-H. Yang, T.Y. Koo and Y.H. Jeong
**Room-temperature Ferromagnetism in the Bi Transition-metal-oxideBilayer BiMnO$_3$/BiFeO$_3$** JKPS 2009 55:80-83. [초록]

DeukYong Lee, Jung-Eun Cho, Myung-Hyun Lee, Nam-Ihn Cho and Yo-Seung Song
**Insertion of a TiO$_{2}$ Buffer Layer for the Fixation ofElectrospun TiO$_{2}$ Nanofibers on Glass Substrates** JKPS 2009 55:84-88. [초록]

Jung-Hwan Hyung, M.Shaheer Akhtar, Dong-Joo Kim[illegible] Yang
**electrodes** : 전극, 용접봉
**ZnO-nanowire-covered TiO$_{2}$ Thin-film Electrodes for Improvingthe Photovoltaic Properties of Dye-sensitized Solar Cells** JKPS 2009 55:89-93. [초록]

S.-H. Park, C.-H. Kwak, S.-Y. Seo, S.-H. Kim, B.-H. Kim, C.-I. Park, Y.-W. Park and S.-W. Han
**A Large Quantity of ZnO Nanorods Grown at Room Temperature** JKPS 2009 55:94-97. [초록]

Journal of the Korean Physical Society, Vol. 55, No. 1, July 2009, pp. 72∼75

# Flexible Organic Thin-film Transistors for Photodetectors

Jae-Hong Kwon, Sang-Il Shin and Chang-Hoon Kim
*Display and Nanosystem Laboratory, College of Engineering, Korea University, Seoul 136-713*

In-Kyu You and Gyeong-Ik Cho
*Research Laboratory/Flexible Devices Team, Convergence and Components & Materials, Electronics and Telecommunications Research Institute, Daejeon 305-700*

Byeong-Kwon Ju*
*School of Electrical Engineering, College of Engineering, Korea University, Seoul 136-713*

(Received 26 August 2008)

In this paper, we report on organic thin-film transistors (OTFTs) fabricated on plastic substrates by using 6,13-bis(triisopropylsilylethynyl)pentacene (TIPS-pentacene) as an organic semiconductor and cross-linked poly-4-vinylphenol as the gate dielectric. From these devices, we obtained exemplary I-V characteristics in the dark. We observed that the TIPS-pentacene-based OTFTs showed an efficient photo-current response under illumination with a halogen lamp. From these electrical properties, we found that the threshold voltage and the on-current were about –6 V and $6.65 \times 10^{-7}$ A, respectively, in the dark. However, after illumination, the threshold voltage and the on-current were 3.9 V and $1.32 \times 10^{-6}$ A, respectively.

PACS numbers: 72.80.Le, 73.61.Ph
Keywords: Organic thin-film transistor, 6,13-bis(triisopropylsilylethynyl)pentacene, Cross-linked poly-4-vinylphenol, Photodetector

## I. INTRODUCTION

Organic thin-film transistors (OTFTs) have been studied extensively in recent years because of their potential applicability in low-cost, and disposable plastic electronic products such as integrated circuits [1,2], flexible displays [3,4], smart cards, radio frequency identification (RFID) tags [5,6], and sensors [7–9]. Moreover, OTFT-based applications are inevitable because of their being lightweight and their having low power consumption, low operating voltage, and compatibility with diverse substrates. These OTFTs are available in a cost-effective way and are scalable to large areas similar to the roll-to-roll process using an available solution process.

OTFTs with photosensitive organic semiconductor (OSC) materials can be used as organic phototransistors, key components of optoelectronic circuits, allowing the detection of light and photo-switching. In particular, OTFT based sensors are active devices. Namely, different electronic parameters of the devices can be extracted from their electrical characterization. Therefore, they are multi-parametric sensors and offer the possibility of using a combination of variables in order to characterize their response to the parameter to be sensed. In this paper, we present a solution-processed OTFT on a plastic substrate and the basics of a concept based solely on OTFTs used as the sensing element without the need of any additional sensor element.

## II. EXPERIMENTS

We fabricated devices with a bottom-gate top contact [10] as shown in Fig. 1(a). Polyethersulfone (PES) films, 100-$\mu$m-thick, were used as flexible substrates and were fabricated on a 150-nm-thick indium-tin oxide (ITO, sheet resistance ∼10 Ω/□) gate electrode, which was sputtered on a 100-$\mu$m-thick PES substrate. Sequentially, a poly-4-vinylphenol (PVP) film served as a gate dielectric. To prepare the PVP solution, we mixed the PVP powder (Sigma-Aldrich, Mw: ∼20,000) with 13 wt% propylene glycol monomethyl ether acetate (PGMEA). We, then, added the cross-linking agent, poly melamine-co-formaldehyde methylated (Sigma-Aldrich, Mw ∼511), to the PVP solution in a ratio of 1 : 20. To form a PVP dielectric film, we coated the PVP solution on the PES substrate with an ITO electrode. The curing process was conducted at 200 °C for 10 min on a hot plate to enforce

*Corresponding Author: bkju@korea.ac.kr; Tel: +82-2-3290-3237; Fax: +82-2-3290-3791; URL: http://diana.korea.ac.kr

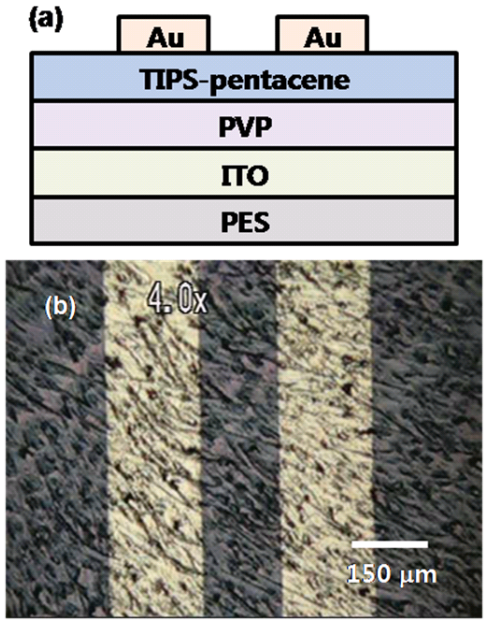


Fig. 1. (a) Cross-sectional diagram of the OTFT's structure. (b) Optical micrograph of our TIPS-pentacene and PVP-based OTFT fabricated on a PES substrate.

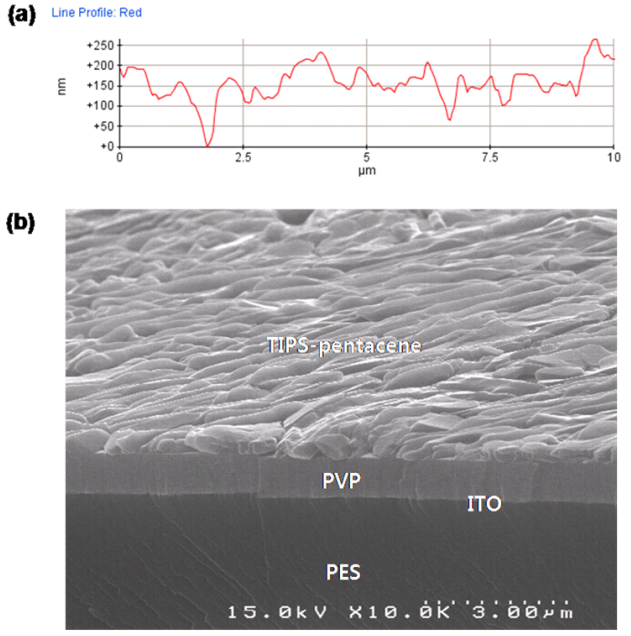


Fig. 2. (a) AFM line profile of the TIPS-pentacene surface film. (b) Cross-sectional FE-SEM micrograph of the flexible TIPS-pentacene-based OTFT structure.

the cross-linking of the PVP polymer. Next, the 6,13-bis(triisopropylsilylethynyl)pentacene (TIPS-pentacene, Hanafine Chem. Co.) film was formed by drop casting from an 8 wt% solution of TIPS-pentacene in tetraline. The coated TIPS-pentacene-based device was annealed using a hotplate at 110 °C for 2 min. Finally, gold (Au, 200 nm thickness) source/drain electrodes were deposited by using thermal evaporation (DOV Co., Ltd.). Also, a shadow mask was used to define the source and the drain electrodes. The channel width and length were 1500 $\mu$m and 150 $\mu$m, respectively. An optical micrograph of our TIPS-pentacene and PVP-based OTFT fabricated on a PES substrate is shown in Fig. 1(b). After device fabrication, the transistor characteristics were measured using a semiconductor characterization system (Keithley SCS/4200). We observed the surface morphology using an atomic force microscope (AFM; Veeco, Dimension 3100).

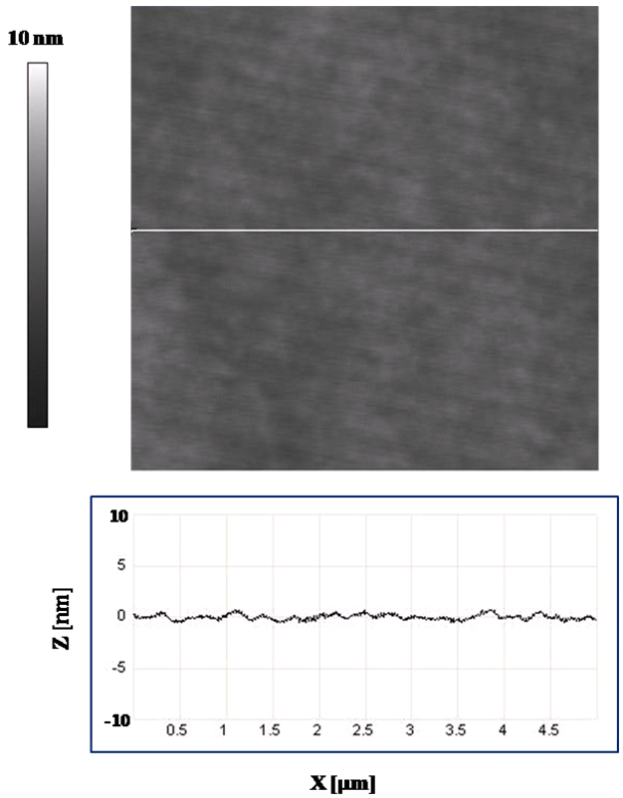


Fig. 3. AFM image and $z$-axis line-scan profiles of PVP-coated ITO/PES substrates (scan area: $5 \times 5$ $\mu$m$^2$).

## III. RESULTS AND DISCUSSION

In our work, we fabricated a simple top contact OTFT by using TIPS-pentacene as the OSC and PVP as the gate dielectric, as shown in Fig. 1(a). Fig. 2(a) shows an AFM line profile of the TIPS-pentacene surface film (root-mean-square (RMS) roughness: 42.29 nm). Fig. 2(b) shows a cross-sectional field-emission scanning electron microscope (FE-SEM) image of the structure for a flexible TIPS-pentacene-based OTFT with a PVP gate dielectric.

Figure 3 shows an AFM image and $z$-axis line-scan profile of PVP-coated ITO/PES substrates. As expected

Table 1. Summary of the flexible TIPS-pentacene-based OTFT's characteristics in the dark and under light.

| | Threshold voltage [V] | Subthreshold slope [V/dec] | Off current | On current | Mobility [$cm^2$/Vs] |
|---|---|---|---|---|---|
| In dark | –6.0 | 6.85 | $9.32 \times 10^{-11}$ | $6.65 \times 10^{-7}$ | $8.2 \times 10^{-3}$ |
| In light | 3.9 | 1.34 | $4.8 \times 10^{-10}$ | $1.32 \times 10^{-6}$ | 0.01 |

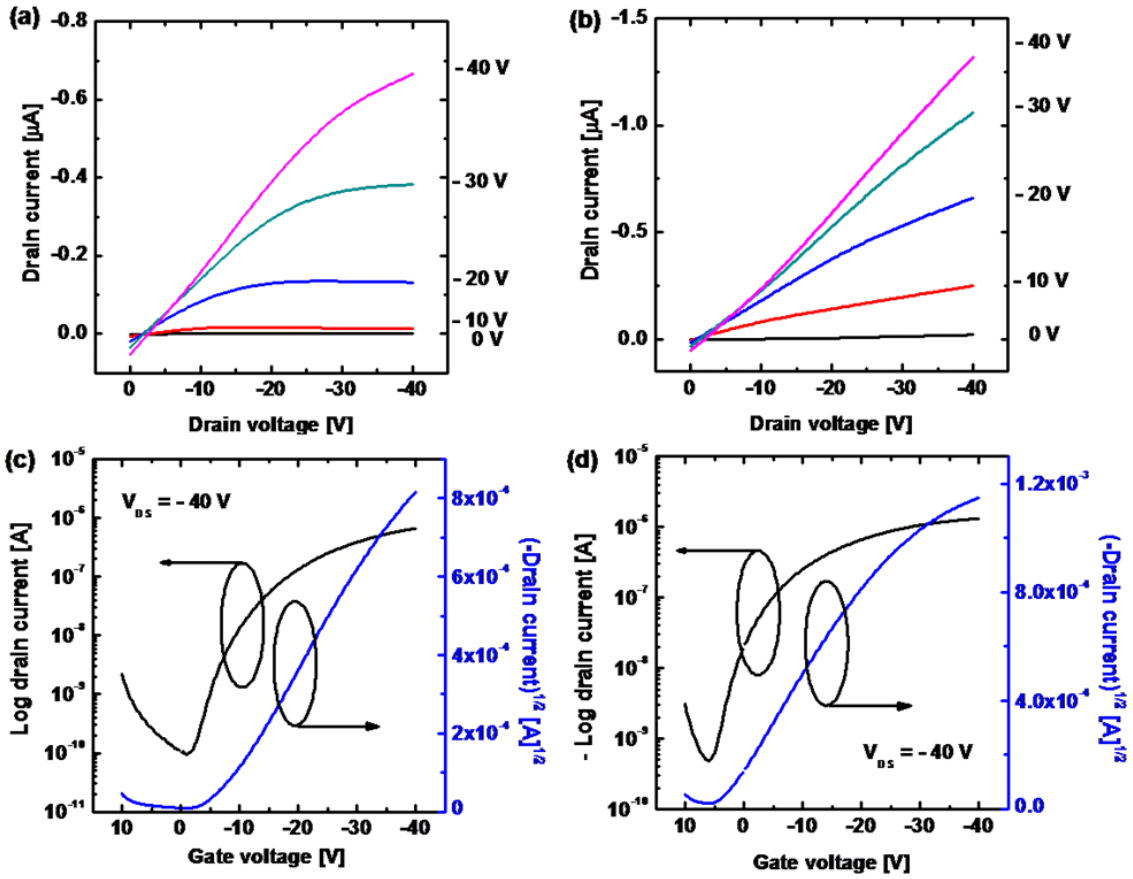


Fig. 4. Output characteristics of flexible TIPS-pentacene-based TFTs with PVP gate insulators (a) in the dark and (b) illuminated at 15 mW/$cm^2$. Transfer characteristics of the devices (c) in the dark and (d) illuminated at 15 mW/$cm^2$.

from the observations in Fig. 3, the surface characteristic is very smooth, and the RMS roughness of the surface is 0.347 nm. These smooth surface characteristics lead to superior insulator properties for the gate dielectric layer and play a significant role in the excellent performance of the resulting OTFT due to the more well-ordered molecular structure on the gate dielectric layer. The relationship between the molecular ordering of the gate dielectric layer and the electrical characteristics of the device has recently been extensively investigated [11]. If the dielectric film has poor surface roughness, then this roughness leads to valleys in the channel region. These valleys may act as carrier traps with a number of scatterings [12]. If we consider the holes located in the rough valleys at the dielectric, the source-drain field only supports drift movement along the surface and cannot support a charge movement out of the rough valley away from the surface. In additional, in accumulation (Gate voltage, $V_G < 0$ V), the gate field opposes any movement of charges away from the dielectric interface. The holes are "trapped" in the roughness minima and can only move out by diffusion or by drift along a local horizontal potential gradient caused by roughness variations [13]. Therefore, improving the surface properties of the gate dielectric layer should be considered as a way to achieve high field-effect mobility.

Figure 4 shows the electrical characteristics of flexible OTFT devices fabricated with TIPS-pentacene and PVP on PES substrates. The output characteristics in the dark are shown in Fig. 4(a). The electron accumulation mode is achieved with a negative bias gate voltage, showing a typically a *p*-type transistor behavior. As shown in Figs. 4(a) and (b), the positive current near a 0 V drain bias, increasing with $V_G$, is the result of the leakage current through the gate-dielectric layer between the source-drain and gate electrodes [14]. Fig. 4(c) shows

the OTFT transfer characteristics in the dark. Figs. 4(b) and (d) show the output and the transfer characteristics of the OTFT, respectively, at illumination. These curves show a photo-response at a white light intensity (halogen lamp) of 15 mW/cm$^2$. We can see that light from the lamp is absorbed mainly in the range of wavelengths of approximately 475 – 525 nm (2.6 – 2.4 eV). A related measure is the ratio of the total drain current under illumination to the drain current in the dark, which is refered to as the photo-response ($R_{L/D}$) and is defined as [15]

$$R_{L/D} = \frac{I_{Dillum}}{I_{Ddark}} \quad (1)$$

In the following, photo-response of our device is approximately 5.15 at 15 mW/cm$^2$. As expected, for field-effect transistors, the output characteristics show two distinct regions of device operation, linear and saturation. The non-ideal behavior of the device in the linear region (at low $V_{DS}$) is most likely due to the current crowding associated with the contact resistance between the OSC channel and source the and drain electrode [16]. Fig. 4(d) shows the gate-voltage-induced electron-enhanced region. In the depletion region, the drain-source current ($I_{DS}$) at illumination increases more than $I_{DS}$ in the dark. The increase in $I_{DS}$ can be explained by the generation of a large number of charge carriers due to the photo-induced charge transfer at the OSC. Also, the threshold voltage for reaching the accumulation mode and the opening of the transistor shifts to lower values upon illumination (*i.e.*, a shift from a negative to a positive voltage, see Figs. 4(c) and 4(d)), suggesting that the trap carrier density in the channel is enhanced by photo-doping; moreover, the apparent subthreshold swing is increased. From Figs. 4(c) and (d), we see that the magnitudes of the off and on state drain currents, for illumination are larger than the off and on state drain currents in the dark. In other words, when illumination is generated, the drain current is increased because the photo-generation rate of the excitons (and therefore the charge carriers) in the channel of the device increases as the illumination is generated. The electrical parameters were extracted from Figs. 4(c) and (d) and are listed along with other device characteristics in Table 1.

## IV. CONCLUSIONS

In this paper, we described fabrication of a solution-processed OTFT on a plastic substrate and the change in the electrical characteristics of a photo-responsive device. We explained the increase in the drain and the source currents upon illumination by the generation of a large carrier concentration due to photo-induced charge transfer at the OSC. Here, we observed the basics of a concept for a photo-responsive flexible OTFT with TIPS-pentacene for the OSC and PVP for the gate dielectric without any additional sensing elements. We forecast that the simplicity and the low cost of this OTFT fabrication technique, as well as its adaptation to photo-sensor manufacture, well provide a very promising technology for industry.

## ACKNOWLEDGMENTS

This work was supported by the National Research Laboratory (NRL, R0A-2007-000-20111-0) Program of the Ministry of Science and Technology (Korea Science and Engineering Foundation), Industrial-Education Co-operation Program between Korea University and L.G. Display Co. Ltd., and the IT R & D program of Ministry of Knowledge Economy of Korea (MKE, 2008-F024-01, Development of Mobile Flexible IOP Platform).

## REFERENCES

[1] S. K. Park, J. E. Anthony and T. N. Jackson, IEEE Elec. Dev. Lett. **28**, 877 (2007).
[2] B.-H. Lee and H. J. Kim, J. Elec. Eng. Tech. **2**, 373 (2007).
[3] H. Y. Cheng, C. C. Lee, T. S. Hu and J. C. Ho, J. Korean Phys. Soc. **48**, S115 (2006).
[4] Y. K. Moon, S. H. Kim, D. Y. Moon, W. S. Kim and J. W. Park, J. Korean Phys. Soc. **51**, 1732 (2007).
[5] T. W. Kelley, P. F. Baude, C. Gerlach, D. E. Ender, D. Muyres, M. A. Haase, D. E. Vogel and S. D. Theiss, Chem. Mater. **16**, 4413 (2004).
[6] J. Kim, D. Kim, J. Burm, K. Chang and Y. J. Yoon, J. Korean Phys. Soc. **53**, 831 (2008).
[7] S. Uttiya, T. Kerdcharoen, S. Varanayon and S. Prayontep, J. Korean Phys. Soc. **52**, 1575 (2008).
[8] J.-Y. Kim, T.-Z. Shin and M.-K. Yang, J. Elec. Eng. Tech. **2**, 408 (2007).
[9] I. Graz, M. Kaltenbrunner, C. Keplinger, R. Schwödi auer, S. Bauer, S. P. Lacour and S. Wagner, Appl. Phys. Lett. **89**, 073501 (2006).
[10] D. Park, J. Heo, J. Kwon and I. Chung, J. Korean Phys. Soc. **54**, 687 (2009).
[11] Y. Jang, D. H. Kim, Y. D. Park, J. H. Cho, M. Hwang and K. Cho, Appl. Phys. Lett. **87**, 152105 (2005).
[12] D. K. Hwang, W. Choi, J. M. Choi, K. Lee, J. H. Park, E. Kim, J. H. Kim and S. Im, J. Electochem. Soc. **154**, H933 (2007).
[13] S. Steudel, S. D. Vusser, S. D. Jonge, D. Janssen, S. Verlaak, J. Genoe and P. Heremans, Appl. Phys. Lett. **85**, 4400 (2004).
[14] J.-H. Kwon, J.-H. Seo, S.-I. Shin, K.-H. Kim, D. H. Choi, I. B. Kang, H. Kang and B. K. Ju, IEEE Trans. Electron Devices **55**, 500 (2008).
[15] M. C. Hamilton, S. Martin and J. Kanicki IEEE Trans. Electron Devices **51**, 877 (2004).
[16] R. R. Troutman and A. Kotwal, IEEE Trans. Electron Devices **36**, 2915 (1989).